PHYSICAL REVIEW B VOLUME 26, NUMBER 2 15 JULY 1982

Electronic structure of nickel silicides Ni_2Si, NiSi, and $NiSi_2$

A. Franciosi and J. H. Weaver
Synchrotron Radiation Center, University of Wisconsin-Madison, Stoughton, Wisconsin 53589

F. A. Schmidt
Ames Laboratory, Iowa State University, Ames, Iowa 50011
(Received 7 January 1982)

Synchrotron-radiation photoemission studies of bulk samples of Ni_2Si, NiSi, and $NiSi_2$ show valence-band emission dominated by Ni $3d$—derived features. These d bands shift toward E_F and broaden with increasing Ni concentration and Ni-Ni interaction, falling at -3.2 eV for $NiSi_2$ and -1.3 eV for Ni_2Si. In each case, the density of states near E_F is very low. These results are interpreted in terms of recent calculations which are shown to forecast correctly the general trends and modifications of the silicide electronic structure. Further, they indicate that the d-band features observed in photoemission reflect d states which are not directly involved in the Ni—Si bonds. Core-level studies show that charge transfer plays a minor role in the chemical bond, but changes in the electronic configuration account for the observed shifts in the Ni $3p$ binding energy.

The structural and electronic properties of metal silicides are receiving increasing attention in connection with efforts to understand the behavior of reactive Si-metal interfaces.[1] Most transition metals and near-noble-metals can react with silicon at low temperatures or even at room temperature to form thin silicidelike phases.[2–7] The presence of such reaction products at the interface determines the properties of electronic devices and is of paramount importance in the new technology of very large scale integrated circuits.[8]

To better understand chemical bonding at the interface and to identify potential structural and electronic differences between bulk silicides and these silicidelike phases, one must examine both bulk and interface silicides. However, very little is known about the electronic structure of bulk silicides.[9] In this paper we discuss a photoemission investigation of the bulk nickel silicides Ni_2Si, NiSi, and $NiSi_2$. These results have direct bearing on interface studies and they are also important from the point of view of bulk electronic structures of alloys because one rarely has an opportunity to study several stable phases of an alloy and observe systematics in the electronic structure.

The measurements discussed here reveal well-defined trends in the electronic structure of the silicide series and allow us to make comparison with a number of recent density of states calculations. The Ni $3d$—derived band is shown to dominate the valence-band spectra and to vary substantially in binding energy and width when going from Ni_2Si to $NiSi_2$. This trend reflects the reduced d-d hybridization in the Si-rich silicides. Core-level photoemission results show that ionicity plays a minor role in the silicide chemical bond; configuration and possibly relaxation effects explain the observed shifts in binding energies.

EXPERIMENTAL

The samples were prepared by comelting high-purity nickel and silicon in a nonconsumable arc furnace. The melts were made on a water-cooled copper hearth under a purified argon atmosphere. Ni_2Si and NiSi melt congruently and formed relatively large grains; $NiSi_2$ forms peritectically at 980 °C. To ensure that the peritectic reaction was completed, and to enhance grain growth, the $NiSi_2$ casting was heated for five days at 950 °C. Metallographic examination showed the samples to be single phase and analysis verified that they were stoichiometric.

All measurements were performed in an ultrahigh-vacuum photoelectron spectrometer (operating pressure $\leq 4\times10^{-11}$ Torr). Clean surfaces were obtained by fracturing the samples *in situ* and then moving them to the common focus of the monochromatic synchrotron radiation beam and the electron energy analyzer. Details of the experimental system have been given in Ref. 10.

Synchrotron radiation from the 240-MeV electron storage ring Tantalus at the University of Wisconsin-Madison was dispersed by a toroidal grating monochromator, and photoelectron energy distribution curves (EDC's) were recorded with a commercial double-pass cylindrical mirror analyzer. The overall resolution (electrons plus photons) was typically ~ 0.4 eV for the valence-band studies. The Si $2p$ and Ni $3p$ core emission was investigated with photon energies of 120 eV (Si $2p$ with ~ 0.5-eV resolution) and 110 eV (Ni $3p$ resolution only ~ 1 eV).

RESULTS AND DISCUSSION

Photoelectron energy distribution curves for the Ni_2Si valence band are shown in Fig. 1 for photon energies between 12 and 120 eV. The spectra are normalized to the height of the d-band maximum near -1.5 eV and are offset upward for clarity. The corresponding EDC's for NiSi and $NiSi_2$ are shown in Figs. 2 and 3, respectively. Comparison shows that the EDC's exhibit analogous $h\nu$ dependence. For Ni_2Si, the valence-band emission is dominated at low photon energy ($h\nu \leq 17$ eV) by two structures lying 1.5 and 2.7 eV below E_F. With increasing photon energy the 2.7-eV feature becomes less visible, nearly vanishes for $h\nu \simeq 24$ eV and reappears at higher photon energy. The other shifts slightly toward lower binding energy (-1.3 eV). For NiSi the prominent structure near -3 eV varies in relative intensity with $h\nu$ and the second structure at -2.1 eV shifts slightly to lower binding energy (-1.8 eV) and becomes dominant for $h\nu \geq 16$ eV. Comparison of the Ni_2Si and NiSi valence-band spectra to those for $NiSi_2$ shows that the main $3d$ feature is much narrower in $NiSi_2$ and falls at substantially higher binding energy than in the other silicides (centered 3.15 eV below E_F). $NiSi_2$ exhibits a second weak structure at -4.8 eV which, like the deeper features in Ni_2Si and NiSi, appears to be least visible for $h\nu \sim 20-25$ eV. In each silicide the spectral features show very little dispersion[11] for $h\nu \geq 24$ eV. The $h\nu$ variation of the intensity of the deeper feature relative to the main one could reflect final state effects involving states well above E_F.

Calculations of the density of states (DOS) for $NiSi_2$, NiSi, and Ni_2Si have been performed by Bisi and Calandra[12] with a semiempirical linear combination of atomic orbital (LCAO) extended Hückel scheme. Calculations for NiSi were also

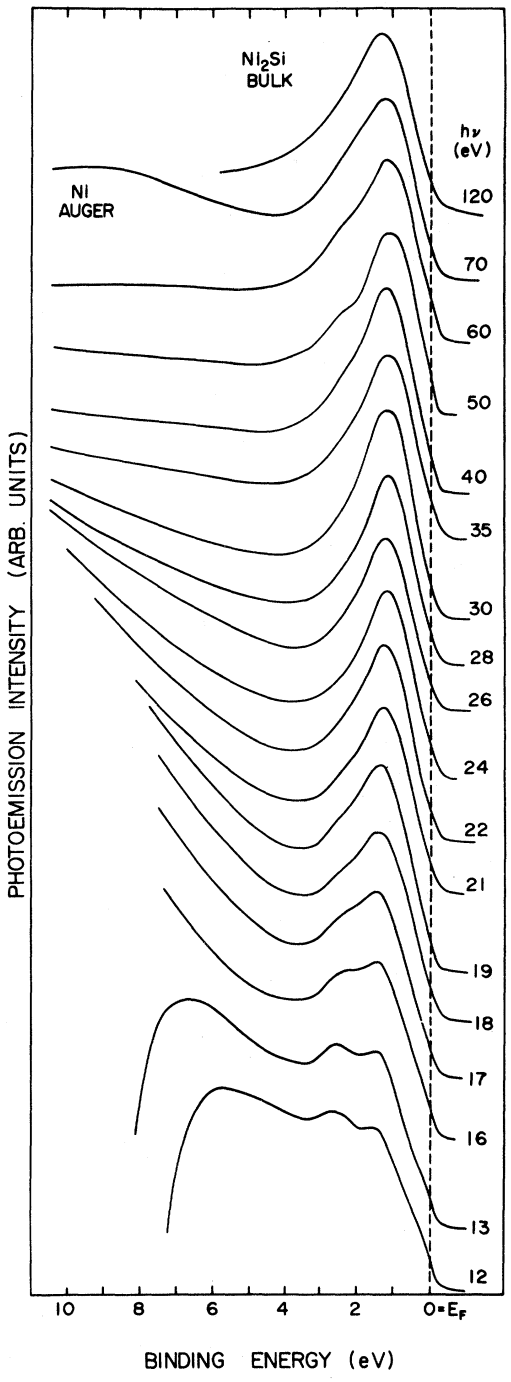

FIG. 1. Photoelectron energy distribution curves (EDC's) for the valence bands of Ni_2Si showing dominant Ni-derived d character. The dominant emission feature at 1.3 eV below E_F exhibits no dispersion with photon energy for $h\nu \geq 20$ eV. It and the higher binding energy shoulder at 2.7 eV are identified with initial state features in the d-derived bands. Auger emission involving the Ni $3p$ core level can be seen for $h\nu = 70$ eV.

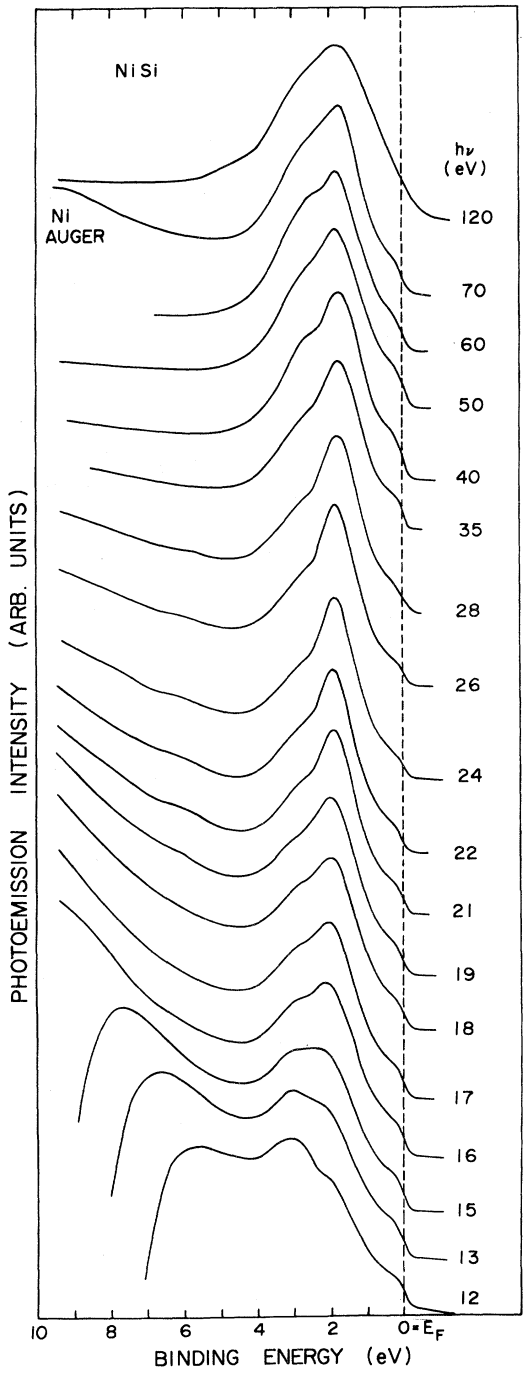

FIG. 2. EDC's for the valence bands of NiSi. The spectra show dominant Ni-derived $3d$ emission features at 1.8 and 3 eV below E_F. The valence states for NiSi appear similar to those of Ni_2Si but with a shift (0.3—0.5 eV) of the $3d$ emission features to higher binding energy and a slight reduction of the $3d$-band width.

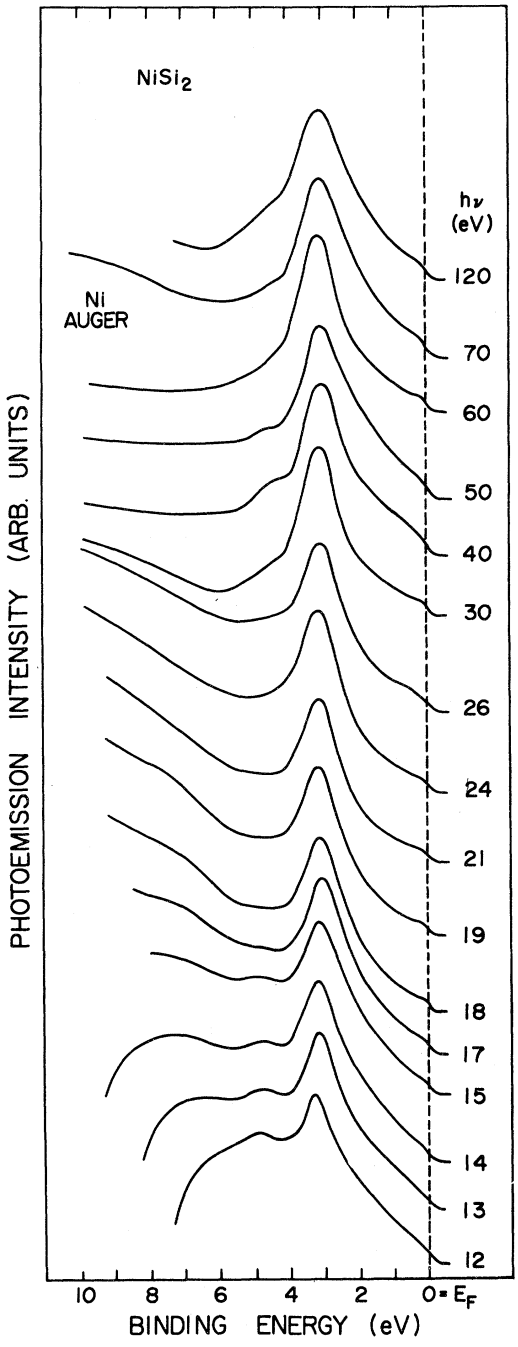

FIG. 3. EDC's for the valence bands of $NiSi_2$. Only one $3d$ emission feature is seen at 3.15 eV below E_F and it exhibits no dispersion with photon energy. The spectra show a substantial reduction of the apparent d bandwidth with respect to NiSi and Ni_2Si and a shift of about 1.9 eV of the main $3d$ emission feature toward higher binding energy. This is due to the reduction of the Ni-Ni interaction in the Si-rich silicide and the subsequent change of Ni $3d$ electronic configuration toward an atomic situation, as discussed in the text.

performed by Boulet *et al.*[13] with a linear muffin-tin orbital (LMTO) scheme. The results of the two calculations for NiSi are in rather good agreement, both showing substantial Si-Ni *p-d* hybridization and an occupied *d*-band width of approximately 6 eV.[12]

In Fig. 4 we reproduce the *d* character of the DOS's calculated by Bisi and Calandra as determined by projecting the $l=2$ state density from the total density of states. The shaded areas represent those portions of the DOS where there is substantial coupling of the Ni *d* and Si *p* states in bonding combination as observed in Ref. 12. Analysis of the calculated DOS's shows that these hybridized states dominate the chemical bonding of the silicides.[12] The major structures which lie closer to E_F (centered $2-3$ eV below E_F) reflect $3d$-derived states which are not directly involved in Ni—Si bonding. The features corresponding to the antibonding Ni d—Si p states lie near and above E_F. For brevity, we will refer to these portions of the *d* DOS as the bonding, nonbonding, and antibonding regions. As is evident from Figs. 1—4, the experimental spectra observed for $15 \leq h\nu \leq 120$ eV reveal the nonbonding portions of the *d* bands. At lower photon energy (e.g., $h\nu=12$ eV), the prominent feature at -3 eV emphasizes contributions from the deeper portion of this nonbonding *d*-band manifold. Since these bands are not involved in the chemical bond, their modification in going from Ni_2Si to $NiSi_2$ is primarily a consequence of the decrease of the Ni-Ni *d-d* interaction in the Si-rich silicides, with only secondary effects from Ni-Si interactions.

Direct comparison of theory with experiment comes through examination of the DOS and the experimental spectra as shown in Fig. 4. Because the results vary only slightly for $h\nu \geq 25$ eV, spectral features in them can be associated with structures in the density of states. In this photon energy range, the Ni $3d$ photoionization cross section is dominant and the EDC's are best compared to the *d* partial DOS. From Fig. 4 one can see immediately that the calculations reproduce the trends in the electronic structure quite well, most notably the movement and changing width of the *d* bands with stoichiometry.

The calculations for Ni_2Si are in quite good agreement with the experimental results of Fig. 4. Taking into account lifetime broadening and experimental resolution, theory would predict that two structures would be observed at about -1.9 and -3.4 eV; experimentally, we find the main peak at

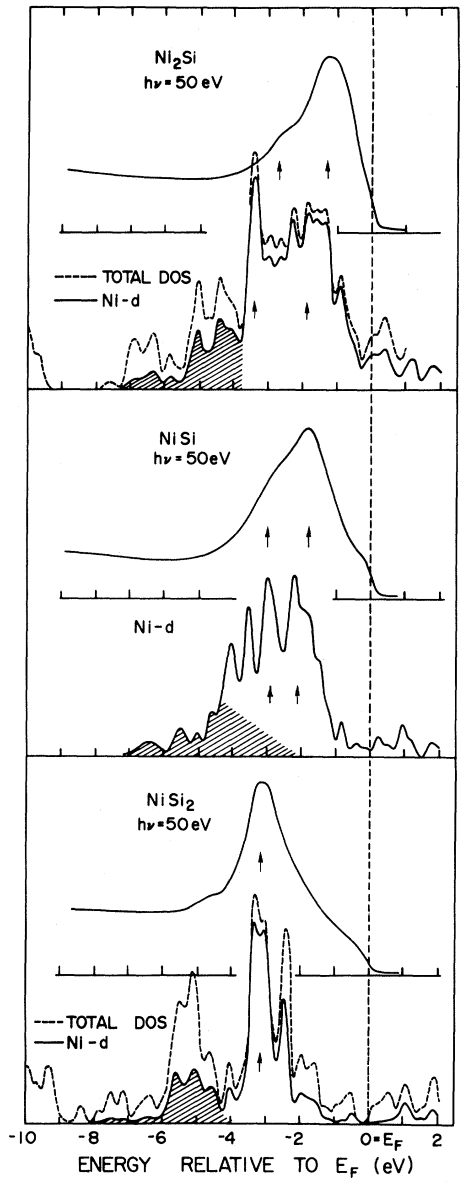

FIG. 4. Comparison of EDC's at $h\nu=50$ eV for Ni_2Si, NiSi, and $NiSi_2$ with density of states calculations from Bisi and Calandra (Ref. 12). At this photon energy, final-state effects are negligible and the spectra mainly reflect the nickel *d* character due to the favorable photoionization cross section of the $3d$ states. Ni *d* character also dominates the calculated DOS as can be seen for Ni_2Si and $NiSi_2$ where we compare the total DOS and the *l*-projected DOS associated with the Ni *d* character (Ref. 12). The shaded regions represent states that are involved in the chemical bond through hybridization with Si *p* orbitals in bonding combination as calculated in Ref. 12. The arrows represent the dominant DOS features and experimental features.

-1.3 eV with the second appearing at -2.7 eV (better seen in Fig. 1 at low photon energy). Theory seems to predict slightly larger (0.6–0.7 eV) binding energies than is actually observed. In our experimental spectra we find no evidence for the bonding states shown shaded in Fig. 4. One could speculate that these are hybridized and have substantially lower photoionization cross sections than do the pure d states, but no conclusive calculations are available to predict modifications in photoionization cross sections associated with hybridization.

Calculations and experiment also agree quite well for NiSi, taking into account lifetime broadening and experimental resolution. Theory predicts[12] a main $3d$ feature at -2.1 eV and a second structure near -2.9 eV (-1.8 and -2.8 eV, respectively, in Ref. 13) and experiment reveals corresponding energies of -1.8 and -3.0, respectively. As for Ni_2Si, there would be improved agreement if the calculated states of Ref. 11 were shifted toward E_F by ~ 0.2 eV.

The agreement of theory and experiment is remarkably good for $NiSi_2$. Here the decrease in the Ni-Ni interaction substantially reduces the d bandwidth and consequently the splitting of the Si p–Ni d bonding and antibonding states. The antibonding states are actually below E_F and theory predicts[12] a substantial amount of d-p hybridization for states within ~ 2.5 eV of E_F. The corresponding bonding states fall ~ 5 eV below E_F and the experimental spectra for $NiSi_2$ do show structure at approximately -5 eV, perhaps because the Ni d character is substantially reduced compared to Ni_2Si or NiSi (fewer d electrons in proportion to Si sp character). The binding energy of the main $3d$ feature (3.15 eV) and the apparent full width at half-maximum (FWHM) are in extremely good agreement with the calculations.[12]

Spectra for the Si $2p$ core levels and the Ni $3p$ cores are shown in Fig. 5. The measured Si $2p$ feature reflects a barely resolved spin-orbit split doublet ($2p_{1/2,3/2}$ splitting 0.6 eV) with a binding energy of 99.39 ± 0.12 eV for the main feature. The Ni $3p$ doublet have binding energies of 65.34 ± 0.25 and 66.93 ± 0.25 eV.[14] In Table I we summarize the experimental binding energies for these $2p$ and $3p$ cores and compare them to the elemental values. The binding energies for elemental Ni [65.7 and 67.4 ± 0.3 eV (Ref. 15)] and Si [99.16 and 99.77 ± 0.10 eV (Ref. 16)] measured relative to the Fermi level of intrinsic bulk Si are given by arrows adjacent to the energy scale of Fig. 5. For

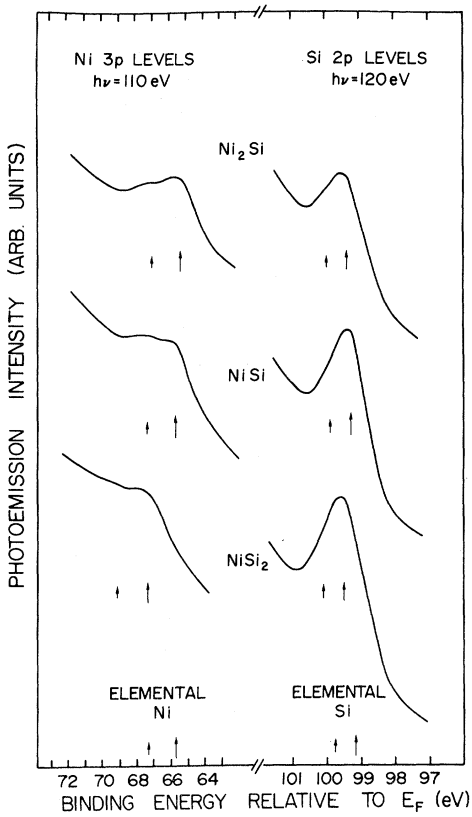

FIG. 5. EDC's showing emission from the Ni $3p$ and Si $2p$ core levels (Ref. 14). The arrows near the energy scale represent literature data of the core binding energies in elemental Ni (Ref. 15) and Si (Ref. 16). Little variation of the binding energy is seen for the Si $2p$ level, while the $3p$ levels move in concert with the $3d$ valence-band features shown in Figs. 1–3 and show that the Ni configuration becomes more atomiclike with increasing Ni dilution in silicon.

the Si $2p$ there is only a very small (if any) shift to higher binding energy in these three silicides. The energy shift of the Ni $3p$ core, however, seems to change in sign and magnitude in the silicide series. For $NiSi_2$ and NiSi, we observe a small negative shift with magnitude comparable to the rather large experimental uncertainty, but we observe an extremely large positive shift for $NiSi_2$ (1.6 eV).

Comparison of the behavior of the main $3d$ emission feature and the $3p$ binding energy for Ni_2Si, NiSi, and $NiSi_2$ shows that these features move in concert: In going from Ni_2Si to NiSi (to $NiSi_2$), the $3p$ core shifts -0.33 (-1.96) eV while the main $3d$ line shifts -0.5 (-1.85) eV. However, as shown in the last two columns of Table I, the calculations indicate charge transfer of only 1% of the valence charge per atom for all stoi-

TABLE I. Binding energies E_B (Ref. 14) for the Ni $3p$ and Si $2p$ levels in Ni metal (Ref. 15), Ni_2Si, NiSi, and $NiSi_2$ and elemental Si (Ref. 16). The binding energies are referred to E_F. Columns 2 and 4 show the measured binding energy shift, ΔE_B, of the cores with respect to elemental Ni and silicon. The last two columns on the right represent the charge transfer Δq (in electrons/atom) as calculated by Bisi and Calandra (Ref. 12) for the three silicides. The calculated charge transfer is always very small ($\leq 1\%$ of the valence charge/atom) and does not explain, even qualitatively, the observed behavior.

	E_B(Ni $3p_{3/2}$)	ΔE_B(Ni $3p$)	E_B(Si $2p$)	ΔE_B(Si $2p$)	Δq(Ni) (e/atom)	Δq(Si) (e/atom)
Ni	65.7	0			0	
Ni_2Si	65.34	-0.36 ± 0.39	99.39	0.23 ± 0.15	-0.037	$+0.074$
NiSi	65.67	-0.03 ± 0.39	99.28	0.12 ± 0.15	-0.054	$+0.054$
$NiSi_2$	67.3	$+1.60\pm0.39$	99.49	0.33 ± 0.15	-0.082	$+0.041$
Si			99.16	0		0

chiometries, in agreement with what might be inferred from the electronegativity scale and consistent with the near-invariance of the Si $2p$ binding energy.[17]

We propose that large variations in the Ni-Ni interaction and corresponding changes in the electronic configuration of the metal atoms account in large measure for the observed behavior in the Ni $3p$ and $3d$ levels in these silicides. In going from Ni_2Si to $NiSi_2$, the spatial density of the Ni atoms changes from $\sim 70\%$ to $\sim 25\%$ of the bulk Ni density. This atomic density is compared to the Ni nearest-neighbor (NN) distance and coordination numbers in Table II where we see that the Ni NN distance is only slightly larger in Ni_2Si and NiSi than in Ni metal while in $NiSi_2$ the NN distance is increased by 53% compared to Ni (the coordination number for Ni_2Si and NiSi decreases substantially relative to Ni metal; in $NiSi_2$ the Ni atoms occupy an fcc metal sublattice as in fcc Ni). This suggests that the Ni d character becomes more atomiclike as the Ni concentration decreases. Calculations confirm this trend toward the atomic configuration, showing the electronic configuration

TABLE II. Structural data for Ni metal, Ni_2Si, NiSi, and $NiSi_2$ from Ref. 27. The first two columns show the structure type and the lattice parameters. In column 3 the spatial density of Ni atoms is given for each structure in units of 10^{-2} atoms Å^{-3}. The data relative to the Ni-Ni distances and coordination in column 4 show that in Ni_2Si each Ni atom has a first "coordination shell" of eight Ni atoms at an average distance of 2.62–2.65 Å (the two values refer to the two inequivalent sites for the Ni atoms in the Ni_2Si structure). In NiSi the coordination decreases to 4 and the average distance increases slightly (2.68 Å). In $NiSi_2$ the first Ni-Ni coordination shell includes 12 Ni atoms at a distance of 3.82 Å with an increase of 53% of the Ni-Ni first neighbor distance with respect to Ni metal.

	Crystal structure	Lattice constants (Å)	Ni atomic density (10^{-2} at. Å^{-3})	Ni-Ni neighbor distance (Å) and number (n)
Ni bulk	fcc	$a=3.52$	9.17	2.49(12) 3.52(6)
Ni_2Si	orthorhombic	$a=5.00$	6.09	2.54(2) 2.59(2) 2.62(1) 2.62(1)
	$PbCl_2$-type	$b=3.73$		2.71(2) 3.44(2)
		$c=7.04$		
				or [a]
				2.54(2) 2.62(1) 2.62(1) 2.71(2)
				2.71(2) 3.63(2)
NiSi	orthorhombic	$a=5.62$	4.11	2.66(2) 2.69(2) 3.34(2)
	MnP-type	$b=5.18$		
		$c=3.34$		
$NiSi_2$	cubic	$a=5.41$	2.53	3.82(12) 5.41(6)
	CaF_2-type			

[a]Two inequivalent sites for Ni atoms in Ni_2Si structure.

of Ni to go from about $3d^{8.7}4sp^{1.2}$ in Ni_2Si to $3d^{8.6}4sp^{1.3}$ in NiSi and to $3d^{8.3}4sp^{1.5}$ in $NiSi_2$.[12] This trend toward more localized, atomiclike Ni d bands is consistent with the results of Figs. 1—4 where the width of the main $3d$ feature is seen to decrease from about 2 to 1 eV (Refs. 18—20) and the d features move to successively higher binding energy.

The $3p$ and $3d$ levels have been observed to shift 11.2 eV to higher binding energy when atomic Ni is compared to the bulk metal.[21,22] Williams and Lang[22] have shown that this shift mainly reflects a superposition of shifts in binding energy due to changing configuration (the distribution of s, p, and d charge from $3d^8 4s^2$ of the free atom to the Ni-metal electronic configuration) and a change due to relaxation of the energy levels due to the creation of the hole in photoexcitation. The analogous change in configuration in these silicides can therefore account for the observed shift of the $3p$ and $3d$ energies (Figs. 4 and 5 and Table I).

Changes in binding energy due to relaxation are probably quite small for the silicides because the one-electron calculations describe the $3d$ states quite well. At least in principle, however, relaxation is certainly modified in the silicide series. In metallic Ni, which has a large density of $3d$ states at E_F, the screening electron has predominantly d character; in the Ni silicides, the $3d$ bands lie deeper and there are very few empty states available for screening at E_F. We believe that this change and the trend toward the atomic $3d^8$ configuration explains why none of these silicides exhibits a d-band satellite.[23] In Ni, the satellite corresponds to a two-hole bound final state for the photoexcitation and requires empty d states at E_F.[24] In the silicides the screening orbital[25] will have mainly sp character, with only minor d contributions and the final state configuration is more likely to be $3d^7$ than $3d^8$.

The results we have presented here show how the electronic structure of the Ni-Si system changes for the three phases Ni_2Si, NiSi, and $NiSi_2$. We have shown that the photoemission results emphasize the nonbonding d character of the valence band, that this d character becomes more atomiclike and sharper in Si-rich silicides, and that it shifts to higher binding energy in concert with the $3p$ core levels of Ni because of the configuration changes. The importance of these configuration effects is considerable because by recognizing them it should be possible to better predict systematics in other alloy systems.[26] The invariance of the binding energy of the Si $2p$ has been used to argue against charge transfer and this was supported by the results of the calculations.[12] Finally, we have shown that the calculations do quite well at predicting the electronic structures. Comparison of these results for bulk silicides with results obtained for Si-Ni interfaces should improve the understanding of interface phases and their electronic properties.

ACKNOWLEDGMENTS

We are extremely grateful to O. Bisi and C. Calandra for stimulating discussions and allowing us to use the results of Ref. 12 prior to publication, F. Cerrina, M. Thuler, and V. L. Moruzzi for illuminating discussions, and the staff of the Synchrotron Radiation Center for cheerful cooperation. One of us (A.F.) would like to thank L. Braicovich for helpful suggestions. The work at the University of Wisconsin was supported by the United States Army Research Office under Grant No. DAAG29-81-K-0140. The Ames Laboratory is supported by the United States Department of Energy under Contract No. W-7405-Eng-82 with Iowa State University. The Synchrotron Radiation Center is supported by the NSF under DMR-8020164.

[1]K. N. Tu and J. W. Mayer, in *Thin Films Interdiffusion and Reaction,* edited by J. M. Poate, K. N. Tu, and J. W. Mayer (Wiley, New York, 1978), Chap. 10; J. Ottaviani, J. Vac. Sci. Technol. 16, 1112 (1979).

[2]I. Abbati, L. Braicovich, and B. De Michelis, Solid State Commun. 36, 145 (1980); G. Rossi, I. Abbati, L. Braicovich, I. Lindau, and W. E. Spicer, *ibid.* 39, 195 (1981).

[3]L. Braicovich, I. Abbati, J. N. Miller, I. Lindau, S. Schwarz, P. R. Skeath, C. Y. Su, and W. E. Spicer, J. Vac. Sci. Technol. 17, 1005 (1980); J. N. Miller, S. A. Schwarz, I. Lindau, W. E. Spicer, B. De Michelis, I. Abbati, and L. Braicovich, *ibid.* 17, 920 (1980).

[4]J. L. Freeouf, G. W. Rubloff, P. S. Ho, and T. S. Kuan, Phys. Rev. Lett. 43, 1836 (1979); P. S. Ho, P. E. Schmid, and H. Föll, *ibid.* 46, 782 (1981).

[5]A. Franciosi, D. J. Peterman, and J. H. Weaver, J. Vac. Sci. Technol. 19, 657 (1981); A. Franciosi, D. J. Peterman, J. H. Weaver, and V. L. Moruzzi, Phys. Rev. B (in press).

[6]P. J. Grunthaner, F. J. Grunthaner, and J. W. Mayer, J. Vac. Sci. Technol. 17, 924 (1980); P. J.

Grunthaner, F. J. Grunthaner, A. Madhukar, and J. W. Mayer, *ibid.* 19, 649 (1981).

[7]W. J. Schaffer, R. W. Bené, and R. M. Walser, J. Vac. Sci. Technol. 15, 1325 (1978); R. W. Bené, R. Walser, G. S. Lee, and K. C. Chen, *ibid.* 17, 911 (1980).

[8]S. P. Murarka, J. Vac. Sci. Technol. 17, 775 (1980).

[9]Photoemission studies of silicides obtained by thin-film reaction can be found in Refs. 2 (Pt_2Si, PtSi), 4 (Pd_2Si), and 6 (Ni_2Si). Studies of bulk silicide samples cleaved *in situ* were performed for VSi_2, $TaSi_2$, and $MoSi_2$ by J. H. Weaver, V. L. Moruzzi, and F. A. Schmidt, Phys. Rev. B 23, 2916 (1981), and for $CrSi_2$ by A. Franciosi, J. H. Weaver, D. G. O'Neill, F. A. Schmidt, O. D. McMasters, O. Bisi, and C. Calandra (unpublished).

[10]G. Margaritondo, J. H. Weaver, and N. G. Stoffel, J. Phys. E 12, 662 (1979).

[11]Figures 1–3 suggest small shifts of the *d*-band maximum if spectra at $h\nu=24$ eV are compared with results for $h\nu\simeq120$ eV. A shift of 0.1–0.15 eV is observed for Ni_2Si while NiSi and $NiSi_2$ exhibit smaller dispersion (0.05–0.08 eV). However, much physical significance should not be attached to these numbers, owing to the difficulty of properly estimating a varying secondary background and of taking into account the effect of a varying experimental resolution, worse ($\sim$0.5 eV) for the high-energy spectra than for the low-energy ones ($\sim$0.3 eV).

[12]O. Bisi and C. Calandra, J. Phys. C 14, 5479 (1982).

[13]R. M. Boulet, A. E. Dunsworth, J.-P. Tan, and H. L. Skriver, J. Phys. F 10, 2197 (1980).

[14]We did not attempt a proper deconvolution of the spin-orbit components of the Si 2*p* and Ni 3*p* doublets. The quoted binding energies correspond to the peak intensities with respect to a linearly extrapolated secondary background. While the Ni $3p_{3/2}$ and Ni $3p_{1/2}$ components can be clearly identified in Fig. 5, the experimental resolution made it impossible to decompose the Si 2*p* doublet. The Si $2p_{1/2}$ component in Fig. 5 is indicated only tentatively through the spin-orbit splitting appropriate for bulk silicon ($\sim$0.6 eV).

[15]S. Hüfner, G. K. Wertheim, and J. H. Wernick, Solid State Commun. 17, 417 (1975); in *Photoemission in Solids II, Vol. 27* of *Topics in Applied Physics,* edited by L. Ley and M. Cardona (Springer, New York, 1978), p. 376.

[16]F. J. Himpsel, P. Heimann, T.-C. Chiang, and D. E. Eastman, Phys. Rev. Lett. 45, 1112 (1980).

[17]If we reference the energy scale to the vacuum level, from the silicide work function and from literature data (Ref. 16), the Si 2*p* binding energy is Si bulk—104.12 eV$\pm$0.2; Ni_2Si—104.2$\pm$0.2; NiSi—104.30$\pm$0.2; $NiSi_2$—104.07$\pm$0.2. Hence very little, if any, chemical shift is observed.

[18]The effect is actually larger since lifetime broadening increases in $NiSi_2$ because the 3*d* hole is deeper in energy with respect to E_F. Two different mechanisms can describe this band narrowing, i.e., the Heine inverse fifth power effect (Ref. 19) which is due only to the increase in atomic separation, and the reduced 3*d* tunneling effect (Ref. 20) in alloys with *sp* elements. The rate at which 3*d* electrons of a given energy tunnel through the $l(l+1)/r^2$ centrifugal barrier from a given site to a nearest-neighbor site is proportional to the density of final states at that energy associated with the nearest-neighbor site (Ref. 19). When Ni nearest neighbors are replaced by silicon atoms, the much lower density of final states leads to narrower *d* bands.

[19]W. Heine, Phys. Rev. 153, 673 (1967).

[20]V. L. Moruzzi, A. R. Williams, and J. F. Janak, Phys. Rev. B 10, 4856 (1974).

[21]D. A. Shirley, R. L. Martin, S. P. Kowalczyk, F. R. McFeely, and L. Ley, Phys. Rev. B 15, 544 (1977).

[22]A. R. Williams and N. D. Lang, Phys. Rev. Lett. 40, 954 (1978).

[23]Y. Baer, P. F. Heden, J. Heldman, M. Klasson, C. Nordling, and K. Seigbahn, Phys. Scr. 1, 55 (1970); C. Guillot, Y. Ballu, J. Paipne, J. Lacante, K. P. Jain, P. Thiry, R. Pinchaux, Y. Petroff, and L. M. Falicov, Phys. Rev. Lett. 39, 1632 (1977); M. Iwan, F. J. Himpsel, and D. E. Eastman, *ibid.* 43, 1829 (1979).

[24]D. R. Penn, Phys. Rev. Lett. 42, 921 (1979); L. C. Davis and L. A. Feldkamp, Phys. Rev. B 23, 6239 (1981).

[25]N. Mårtensson and B. Johansson, Phys. Rev. Lett. 45, 482 (1980); J. C. Fuggle, M. Campagna, Z. Zolnierek, R. Lässer, and A. Platau, Phys. Rev. Lett. 45, 1597 (1980), and references therein.

[26]J. C. Fuggle and Z. Zolnierek, Solid State Commun. 38, 799 (1981).

[27]W. B. Pearson, *Handbook of Lattice Spacing and Structures of Metals and Alloys* (Pergamon, New York, 1958); W. B. Pearson, *The Crystal Chemistry and Physics of Metals and Alloys* (Wiley, New York, 1972).